

NOTE

Preliminary Measurements of the Cryogenic Dielectric Properties of Water–Ammonia Ices: Implications for Radar Observations of Icy Satellites

Ralph D. Lorenz

Lunar and Planetary Laboratory, Department of Planetary Sciences, University of Arizona, Tucson, Arizona 85721-0092
E-mail: rlorenz@lpl.arizona.edu

Received March 10, 1998; revised August 10, 1998

I report preliminary measurements of the complex permittivity of frozen aqueous ammonia solutions at liquid nitrogen temperatures, representative of those in the saturnian system. The real part of the dielectric constant of 30% ammonia ice is around 4.5 at near-DC frequencies and at ~ 1 MHz, compared with around 3.1 for pure water ice. The loss tangents of ammonia-rich ices seem somewhat ($\sim 50\%$) higher than those for water ice, for which the few low-temperature experiments to date indicate values comparable with predictions by Thompson and Squyres (1990, *Icarus* 86, 336–354) and Maetzler (1998, in *Solar System Ices* (B. Schmitt, C. DeBergh, and M. Festou, Eds.), pp. 241–257, Kluwer Academic, Dordrecht), but considerably higher than models by Chyba *et al.* (1998, *Icarus*, in press). Ammonia-rich ice may reconcile the radar and optical appearance of Titan's surface: the detectability of water–ammonia ice on Titan by the Cassini mission and the implications for Titan's origin and evolution are discussed. © 1998 Academic Press

Introduction. The optical and microwave properties of water ice close to its melting point, with a variety of solutes, have received much attention owing to their importance in terrestrial remote sensing. The remarkable transparency of cold (< 260 K) water ice to microwave radiation has been noted in returns from both terrestrial and astronomical targets, leading to both anomalously high backscatter and polarization ratio, although few laboratory measurements of ice dielectric properties at low (< 200 K) temperatures have been made. A key question is whether the substantial presence of ammonia, likely in the saturnian system, significantly modifies these properties.

Figure 1 shows disk-averaged optical ($1 \mu\text{m}$) and radar reflectivities of the Galilean satellites, Titan's brighter hemisphere, and the Moon. Of course, all of the bodies discussed are heterogenous at a variety of scales, but spatially resolved spectral data on Titan are only now becoming available, so these disk-averaged data must serve as the present basis for comparison. It can be seen that the Galileans and the Moon fall on roughly a mixing line—with the position along the line indicating a crude rock:ice ratio. Titan does not fall on the line—evidently it cannot be

considered as a pure rock–ice mixture (see Lorenz and Lunine 1997 for a discussion). It is possible that organic compounds (both liquid and solid) are present on Titan's surface—these may allow it to appear optically bright yet defeat the volume scattering effects that would make an icy surface radar-bright. It has not yet been demonstrated which (or, indeed, whether any) combination of rock, ice, and organics can reproduce the radar and optical reflectivities simultaneously and in a geologically plausible manner.

Another possibility is that Titan's surface has a significant non-water ice component. The possibility that Titan may have incorporated both methane clathrate ice and ammonia hydrate was suggested at an early stage (Lewis 1973). Unlike the jovian subnebula, the saturnian nebula would have been cool enough to incorporate these compounds (e.g., Pollack *et al.* 1976). The fact that methane is present on Titan is consistent with the fact that methane clathrate is incorporated into Titan: since ammonia hydrate has a higher condensation temperature, it, too, should have been included in the growing Titan (see, e.g., Lewis 1973, Consolmagno and Lewis 1978).

According to this scenario, after accretion Titan would have had a water–ammonia ocean, with an ammonia-rich atmosphere above. The initial ammonia atmosphere would have been processed by photolysis (Atreya *et al.* 1978) and/or shock processing (Jones and Lewis 1987) to generate the nitrogen atmosphere we see today: this is a favored model for the formation of Titan's atmosphere (Lunine 1989). As the ocean cooled, ammonia-free ice I would have formed above it (see, e.g., Lunine and Stevenson 1987).

This leaves an ammonia-rich mantle, which could persist as liquid to this day, (e.g., Grasset and Sotin 1997). The 176 K water–ammonia melting isotherm could be only a few tens of kilometers below the surface, and could erupt through cracks in the ice crust which would propagate faster than the ammonia-rich cryomagma in them would freeze (Lorenz 1996). Such events would superimpose ammonia-rich flows over the ice I crust.

Thus, it is entirely plausible that part of Titan's surface may be covered by ammonia-rich ice. This possibility forms the key motivation for this study. In this paper I describe some crude preliminary experiments with water–ammonia ice of various compositions, to determine how the presence of ammonia affects the real and imaginary parts of the complex dielectric constant (hereafter referred to for brevity as the real and imaginary dielectric constant). I compare the measurements with the few literature values for pure ice, and explore the planetary implications.

Sample preparation and observations. Analysis grade ammonia solution (33%) was used in the experiments, together with ordinary tap water.

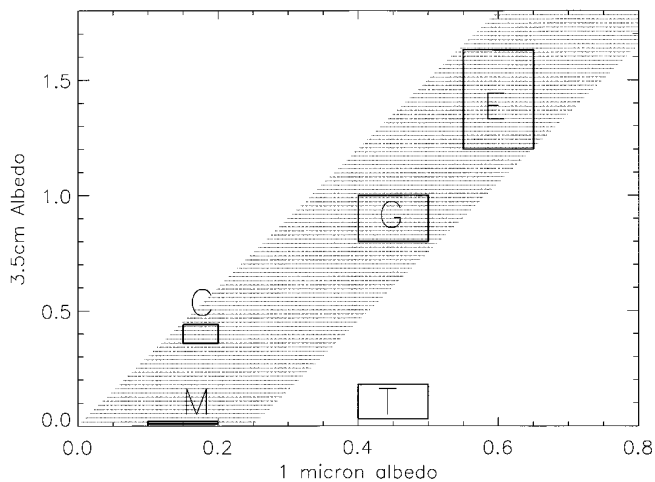


FIG. 1. Optical ($1\ \mu\text{m}$) albedos and radar (same-sense circular polarization) backscatter cross sections for the Galilean Satellites, Titan, and the Moon (indicated by their initials), from the compilation of Lorenz and Lunine (1997). The shaded region indicates a crude mixing line: moving from the Moon through Callisto to Europa increases the ice abundance, with Titan apparently resembling Ganymede at optical wavelengths. Titan's radar reflectivity is much lower than would be expected on this basis, suggesting an additional component.

The fidelity of experiments was not such as to justify using ultrapure reagents, and planetary ices are in any case unlikely to be especially pure. Trace impurities are unlikely to influence comparisons between ammonia-rich and ammonia-poor compositions since Maetzler and Wegmuller (1987) indicate that the effects of ionic impurities are fairly linear. An appropriate mixture of water and ammonia solution was made and frozen between the plates of a parallel plate capacitor by plunging into liquid nitrogen (LN), reaching a temperature of about 77 K. In initial experiments, the capacitor had two 1-mm-thick aluminum plates 5×3 cm, spaced 1 mm apart by a U-shaped nylon sheet, held together by nylon bolts. This capacitor also acted (intermittently, due to leaks) as the sample container. Subsequent experiments used a 12-plate rectangular 15×4.5 cm capacitor, again with 1-mm-thick aluminum plates, spaced by 1-mm nylon washers and held together with nylon bolts: this was placed in a household polyethylene bag and the sample solution was poured in; then the whole assembly was immersed in LN to freeze. The bag method was found to be the most effective way of containing the solution and ice: the thermal stresses upon immersion into LN cracked two trial rigid plastic sample enclosures, although the nylon bolts and washers remained intact.

Previous experiments (e.g., Kargel *et al.* 1991) with freezing ammonia solutions have noted the tendency to supercool and remain as a glass for several minutes or hours. In the present experiments, the freezing and cooling of the sample took only about 20 min (until the vigorous boiling of LN settled), and it may be noted that in the close confines of the parallel plate capacitor there are likely to be many sites for the nucleation of ice crystals, so extensive and prolonged supercooling is unlikely. Electrical properties of water ice samples, monitored by a digital voltmeter (DVM) recording resistance and capacitance, attained their cryogenic values rapidly. Ammonia-rich samples, on the other hand, often changed their properties from those of the room-temperature liquids slowly at first, and then suddenly changed to their cryogenic values. It is conjectured that this phenomenon indicates some supercooling, followed by crystallization. To check that the final state had been reached, one ammonia solution (30%) sample was left in LN overnight: there was negligible (<1%) change in the capacitance reading over 12 hr.

A striking aspect of the sample freezing was that while watery samples formed opaque white ice, with myriad cracks on very small spatial scales, ammonia-rich samples froze into a clear, glassy ice, with relatively few cracks (spaced by typically half to one centimeter).

Electrical measurements. A capacitance measurement C_{meas} records that of the sample cell, plus the cable capacitance C_c which can be determined from open-circuit measurements. The cell capacitance comprises two elements in parallel, C_s due to the sample and the other, C_n , due to other materials between the capacitor plates (in this case nylon spacers).

In the initial experiments, the capacitance of the cell was measured using a commercial DVM (Radio Shack Model 22-174). This instrument uses a timing waveform with a period of 80 msec, so the measurement frequency may be considered ~ 12 Hz. The null (instrument + lead) capacitance was typically 125 ± 10 pF, while the air-filled cell added 60 pF. The component due to the nylon was estimated from the relative areas of the nylon and open areas between the plates. The dielectric constant of the sample material, ϵ_r , is $(C_{\text{meas, sample}} - C_c - C_n) / (C_{\text{meas, air}} - C_c - C_n)$.

The small cell capacitance made the systematic errors in this arrangement very large. However, the consistent trend (thin boxes in Fig. 2) in dielectric constant between pure water and ammonia solutions is apparent, and is unaffected by the systematic errors. This result encouraged the second series of experiments. These experiments used a much larger capacitor, to minimize the systematic effects of lead capacitance. Additionally, the measurements were conducted at a range of radio frequencies, more relevant to radar sounding, and aimed to measure the complex permittivity, so that the absorption loss in the ice can be estimated. This was important also to confirm that the variation in the real part of the dielectric constant was real, and not due to conductivity in the sample (which would masquerade as a higher dielectric constant to the charge-time measurement made by the DVM).

The large capacitor (in effect a nylon-spaced capacitor of ~ 0.6 nF in parallel with a cell capacitance of $0.8\epsilon_r$ nF, with ϵ_r the dielectric constant of the sample material) was measured as before with a DVM for convenience during sample preparation: longer leads increased the null capacitance to 200 pF, but the much higher cell capacitance reduces the systematic errors.

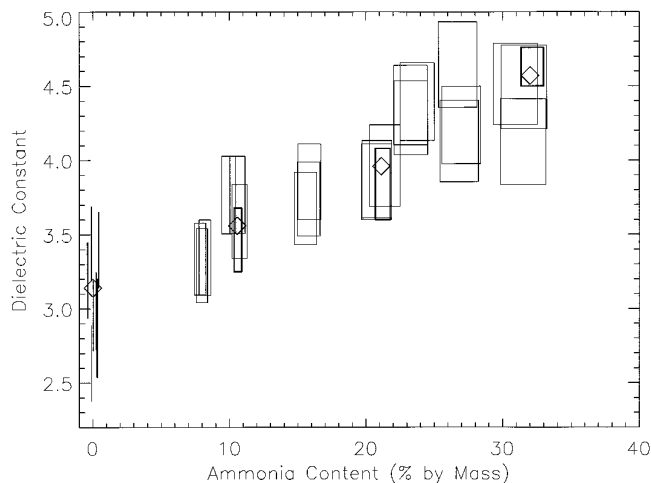


FIG. 2. Real part of the dielectric constant of water-ammonia ice at 77 K as a function of composition. The fine boxes are the initial 12-Hz measurements with the small cell; the thick boxes are those with the large capacitor. Boxes denote estimated uncertainty (there is some uncertainty in composition due to evaporation of ammonia during sample preparation). The diamonds are using the large capacitor at 0.6 MHz.

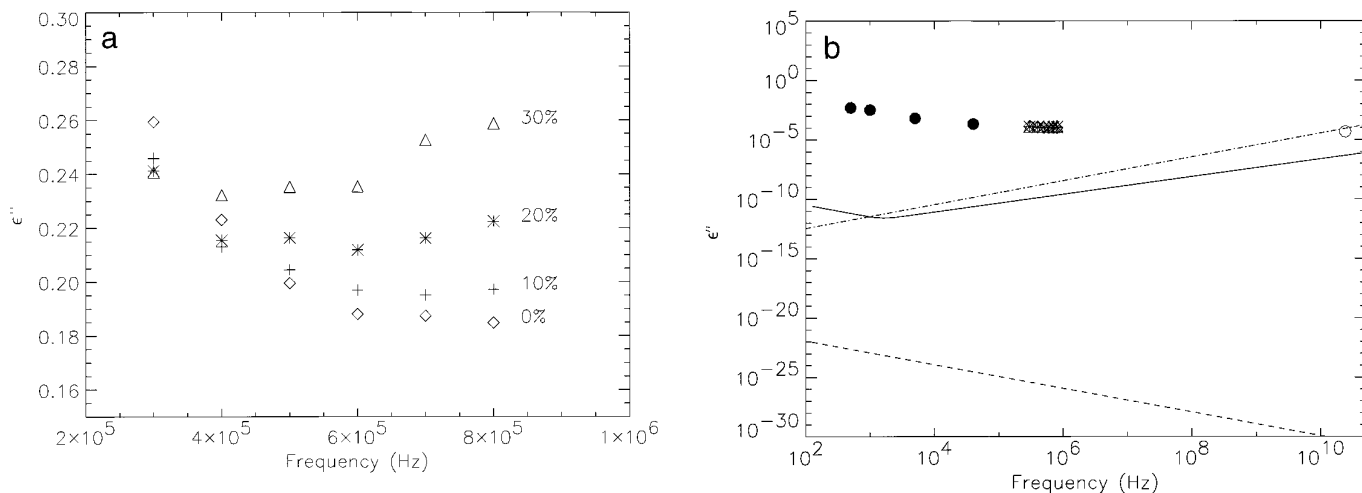


FIG. 3. (a) The present (uncalibrated) measurements of the imaginary dielectric constant. This quantity increases somewhat as the ammonia mole fraction increases, and there is a hint that this increase is stronger at higher frequencies. (b) Complex dielectric coefficient for pure water ice as a function of frequency at 77 K. The solid line is the model of Thompson and Squyres (1990), the dashed line is due to Chyba *et al.* (1998) and the dot-dashed line is due to Maetzler (1998). The open circle is the measurement of Lamb and Turney (1949), the filled circles are from Gough (1972), and the clutch of symbols at about 10^6 Hz shows the present measurements (as from Fig. 3b), but now normalized to 10^{-4} at 1 MHz for the pure water case: the difference between the ammonia-rich and ammonia-poor cases as measured is tiny compared to the differences between model predictions for pure ice, and between the models and most experimental data.

The system accuracy was verified by filling the cell with fluids of known dielectric constant (toluene, $\epsilon_r = 2.4$ at room temperature, and LN, $\epsilon_r = 1.4$): some difficulty was found in reducing the data to obtain these values simultaneously. Coefficients of expansion of the nylon and aluminum components suggest the spacing and area change by only 4% and 1%, respectively. The cell construction was deliberately made very stiff, to preserve the geometry of the plates—expansion of ice on freezing was therefore directed outward between the plates. However, the possibility of some small change in geometry cannot be completely eliminated and the dielectric properties of the nylon may change somewhat with temperature. I therefore discarded the room-temperature calibration and tuned the assumed value of C_n to reproduce the literature value for ice and LN at low temperature, specifically the value of 3.10 determined at 77 K by Gough (1972).

For the more demanding complex dielectric constant measurement, the cell was taken from the preparation laboratory (in a Dewar of LN) to a Hewlett–Packard model HP5371 network analyzer housed inside a faraday cage. After calibration with closed, open, and known loads, this unit measures the complex impedance of the cell over the range 0.3 to a few megahertz. The lower frequency was limited by the analyzer: the upper limit was limited by the lead inductance—measurements above 1–2 MHz were suspect. The HP unit reports the impedance as a resistance and capacitive reactance assumed in series: I convert this into an equivalent resistance and a capacitance (assumed in parallel) using a short iterative scheme. The resistance is converted into a volume resistivity knowing the cell geometry, and thence into the imaginary part of the dielectric constant. Figure 3a shows the estimated imaginary part of the dielectric constant over the frequency range measured for different compositions.

In an attempt to make yet higher frequency measurements, and increase the effective resistance of the cell (and thereby allow the measurement of lower-volume conductivities) a coaxial capacitor geometry was tried. Unfortunately, quantitative interpretation of the resistivity measurements was frustrated by resonances within the capacitor. However, the real part of the dielectric constant of 30% water–ammonia ice at 100–500 MHz was consistent with that measured at lower frequencies. Further, although

no absolute imaginary dielectric constants could be determined, dissipation was evident for the 30% ammonia ice, whereas none could be detected in the pure water ice sample. This is again consistent with the fact that ammoniacal ice is more conductive (lossy) than pure ice. We may note that in the 10–40 GHz range the inversion of the ammonia molecule itself causes strong absorption (e.g., Spilker 1990). As gigahertz frequencies are approached, the wings of this absorption are likely to become a major contributor to losses in any ammonia-bearing medium.

Results and discussion. The results for real dielectric constant are relatively straightforward and robust. Increasing ammonia content increases the dielectric constant, presumably by increasing the polarizability of the ice. The Clausius–Mosotti relationship would indicate that were the polarizabilities equal the slightly denser 30% ammonia ice (approximately the composition of ammonia dihydrate)—with a density of 0.97 g cm^{-3} (Croft *et al.* 1988) compared with ice I (0.92 g cm^{-3} at 77 K)—should have a dielectric constant about 6% higher than that of pure ice, in contrast to the 50% or so I observe here. Thus ammonia hydrate has a much higher polarizability than water ice.

The results for an imaginary dielectric constant of about 2×10^{-1} shown in Fig. 3a could be quantitatively in error, and seem (for pure ice, see Fig. 3b) rather higher than other workers indicate (perhaps due to the impurities in tap water). However, given the consistency of the data and the higher-frequency measurements indicating loss in the ammoniacal sample where none could be measured for the pure ice, the qualitative conclusion that ammonia-doped ice is more lossy than pure ice seems inescapable. It is possible that some of the losses may be due to a residual film of ammonia-rich fluid—brine pockets are probably the major contributor to incremental losses in impure ice (Maetzler and Wegmuller 1987).

Thompson and Squyres (1988) report that no measurements for ammonia-doped ice exist. They also indicate that measurements for pure ice below -60°C are required. In fact some measurements of the latter have been made, although they are somewhat hidden in the literature, and are not mentioned explicitly in Warren's (1984) review. Lamb and Turney (1949) measure the real and imaginary dielectric constants at wavelength 1.25 cm (25 GHz) between about 80 and 270 K. Gough (1972) reports

measurement of the real part of the dielectric constant down to even lower temperatures, at 500 Hz to 1 MHz. That paper also shows figures of the complex capacitance for four temperatures, which may be interpreted to indicate the imaginary dielectric constant. These data are shown in Fig. 3b, along with models by Thompson and Squyres (1988) and Chyba *et al.* (1998), which are both extrapolated from measurements at -60°C and above: a recent model by Maetzler (1998), is also shown. Given the several tens of orders of magnitude difference between the models, the experimental uncertainties—and indeed the difference between pure water ice and ammonia-rich ice—pale into insignificance.

The discrepancy between the Chyba *et al.* (1998) model and the other models and data is striking, but it must be remembered that Fig. 3b shows the dielectric constant at 77 K: according to Chyba (personal communication, 1998) at higher temperatures, where the attenuation is higher, the fit of Chyba *et al.* (1998) to the data of Johari and Charette (1975) is better than that of Thompson and Squyres (1988). It may be noted, however, that the microwave absorption lies between and has contributions from the low-frequency Debye relaxation (e.g., Evans 1965) and the long-wavelength tail of the far-IR lattice absorptions (Hansen, personal communication, 1998) or submillimeter band (Thompson and Squyres 1988). The Chyba *et al.* (1998) model only includes the Debye absorption. While the Chyba *et al.* (1998) model may be useful in specific applications, in general the Maetzler (1998) and Thompson and Squyres (1988) models are preferable.

All the low-temperature experimental data seem to indicate a higher value of the dielectric constant (i.e., a more lossy medium) than the models, although small-sample effects such as parasitic conduction in surface films may be significant in the laboratory measurements: the models are generally extrapolated from large-scale propagation experiments in polar ices. This should be borne in mind when applying centimeter-scale laboratory measurements to kilometer-scale radar sounding on planetary surfaces.

Planetary implications and conclusions. These results are important for the modeling and interpretation of radar data from outer planet satellites. First, while it is known that at low temperatures (below -20°C or so) water ice becomes relatively transparent to microwave and radio wavelength radiation, exactly how transparent determines the depth to which planetary radar measurements sense the surface, and extrapolations from terrestrial temperatures are difficult.

This preliminary investigation has highlighted the fact that the presence of ammonia in ice alters its dielectric behavior, even at very low temperatures. A more detailed laboratory investigation, extending up to higher frequencies (e.g., the Cassini radar operates at Ku band—13.8 GHz) and over a range of temperatures, is warranted. Such an investigation should use a cell with low stray inductance, and platinum electrodes to minimize surface effects, and a better controlled geometry (no spacers).

Despite the crudeness of the present experiments, however, they have demonstrated the following:

1. The real dielectric constant of ammonia-rich ices is significantly (50% for 30% ammonia) higher than that of pure ice.
2. The imaginary dielectric constant is also higher. The difference is only about 50% at 1 MHz, but may be more at shorter wavelengths given the strong absorption of the ammonia molecule at gigahertz frequencies.
3. Extrapolations of higher-temperature water ice data to outer solar system temperatures are fraught with uncertainties. Our results, and those of Lamb and Turney (1949) and Gough (1972), seem to be more in agreement with the modeling of Thompson and Squyres (1990) and Maetzler (1998) than that of Chyba *et al.* (1998). Chyba *et al.*'s principal conclusion, that a European subsurface ocean can be detected by an orbiting radar sounder, is probably still correct since their calculations assumed a significant amount of a lossy impurity (rock) in the European ice crust: e.g., they compute that a subsurface European ocean would be detectable at a depth of 5 km with a 50-MHz radar if the ice has a 10% rock component, corresponding to a loss of about 0.004 db/m, almost all

of which is due to the rock component. For such a loss to be a significant underestimate, the imaginary dielectric constant of ice would need to be higher than about 10^{-4} , or roughly what the laboratory data suggest for ice. The possibility of detecting an ocean at 10–15 km depth, suggested by Chyba *et al.*'s more optimistic models, seems unlikely to be realized.

4. Ammonia-rich ice has a texture different from that of pure ice, at least when both are quenched suddenly on small scales under laboratory conditions.

The implications for Titan are as yet unclear: its anomalous radar appearance may be due to a combination of ices, rocks, and organic material, or it may be due to ammonia in the ice (or indeed to all of these factors). Although on an airless body ammonia hydrate ices might be detected spectroscopically due to absorption at 3300 cm^{-1} ($3.03\text{ }\mu\text{m}$; Fink and Sill 1982) or 5100 cm^{-1} ($1.96\text{ }\mu\text{m}$), 4540 cm^{-1} ($2.202\text{ }\mu\text{m}$), and 1100 cm^{-1} ($9\text{ }\mu\text{m}$; Schmitt *et al.* 1998), on Titan these bands are poorly matched with the deep and complex methane absorptions in its thick atmosphere, such that a space- or ground-based detection is unlikely to be unambiguously achievable. Unfortunately, the Descent Imager/Spectral Radiometer (DISR) carried aboard the Huygens probe (Tomasko *et al.* 1997), which will take spectra at the landing site extends only up to $1.7\text{ }\mu\text{m}$, and so will not be able to detect ammonia in the bands mentioned above.

Cryovolcanic flows on Titan might be morphologically apparent, probably appearing similar to pancake domes on Venus (Lorenz 1996): if radar mapping finds such features, and these features have a larger dielectric constant than the crust on which they are superimposed, then an ammonia–water composition would be indicated. Since roughly 30% ammonia is the peritectic (lowest melting point) composition this material is perhaps the most likely cryolava composition on Titan. The surface electrical properties on Titan may be determined from data from the Huygens probe's radar altimeter. Additionally, if the probe survives impact, the complex permittivity of the upper meter or so of the surface at the probe landing site will be determined by a quadrupole electrode array (Grard 1990) carried as part of the Huygens Atmospheric Structure Instrument (Fulchignoni *et al.* 1997).

It will be useful to study, even in only a disk-averaged sense, the radar properties of other saturnian satellites for comparison. With the possible exception of large Iapetus (and this only using the Arecibo antenna), this is not within the capabilities of ground-based instrumentation. However, the Cassini radar instrument (Elachi *et al.* 1998) may be used in its scatterometer mode to measure the disk-integrated reflectivity of the saturnian satellites from ranges of several tens of thousands of kilometers (its sensitivity is such that the satellite need not necessarily fill the beam). Even though the Cassini radar is some 4 orders of magnitude less powerful, and has 2.5 orders of magnitude less gain than, e.g., the 70-m Goldstone antenna, the range⁴ dependence of radar signal-to-noise ensures that Cassini will be able to perform radar astronomy experiments in the saturnian system, as well as map Titan's surface.

If, for example, other icy satellites like Rhea turn out to have low radar reflectivities (like Titan) but optical remote sensing demonstrates that their rock and organic contents are low—or indeed detects ammonia hydrate directly—then this would lend strong support for the model of the saturnian subnebula's incorporating ammonia, and for the Titan atmosphere's being derived from an ammonia-rich protoatmosphere.

ACKNOWLEDGMENTS

The author acknowledges the support of the Cassini project. Mike Calkins (supported by the Arizona Space Grant program) and Bruno Aguilar assisted with sample and apparatus preparation and measurement, with facilities provided by the TEGA project. Steve Bell assisted with the RF measurements. Chris Chyba is thanked for providing his 1998 paper prior to publication. Referee Gary Hansen is thanked for a number of very useful comments.

REFERENCES

- Atreya, S., T. M. Donahue, and W. R. Kuhn 1978. Evolution of a nitrogen atmosphere on Titan. *Science* **201**, 611–613.
- Chyba, C. F., S. J. Ostro, and B. C. Edwards 1998. Radar detectability of a subsurface ocean on Europa. *Icarus* **134**, 292–302.
- Consolmagno, G. J., and J. S. Lewis 1978. The evolution of icy satellite interiors and surfaces. *Icarus* **34**, 280–293.
- Croft, S. K., J. I. Lunine, and J. Kargel 1988. Equation of state of water–ammonia liquid: Derivation and planetological applications. *Icarus* **73**, 279–293.
- Elachi, C., L. Borgarelli, P. Encrenaz, E. Im, M. A. Janssen, W. T. K. Johnson, R. L. Kirk, R. D. Lorenz, J. I. Lunine, D. O. Muhleman, S. J. Ostro, G. Picardi, F. Posa, L. E. Roth, R. Seu, L. A. Soderblom, S. Vetrella, S. D. Wall, C. A. Wood, and H. A. Zebker 1998. RADAR: The Cassini Titan radar mapper. *Space Sci. Rev.*, submitted.
- Evans, S. 1965. Dielectric properties of ice and snow—A review. *J. Glaciol.* **5**, 773–792.
- Fink, U., and G. T. Sill 1982. The infrared spectral properties of frozen volatiles. In *Comets* (L. Wilkening, Ed.), pp. 164–202. Univ. of Arizona Press, Tucson.
- Fulchignoni, M., F. Angrilli, G. Bianchini, A. Bar-Nun, M. A. Barucci, W. Borucki, M. Coradini, A. Coustenis, F. Ferri, R. J. Grard, M. Hamelin, A. M. Harri, G. W. Leppelmeier, J. J. Lopez-Moreno, J. Am. M. McDonnell, C. McKay, F. M. Neubauer, A. Pedersen, G. Picardi, V. Pirronello, R. Pirjola, R. Rodrigo, C. Schwingenschuh, A. Seiff, H. Svedhem, E. Thrane, V. Vanzani, G. Visconti, and J. Zarnecki 1997. The Huygens atmospheric structure instrument (HASI). In *Huygens: Science, Payload and Mission* (A. Wilson, Ed.), pp. 163–176. ESA SP-1177, European Space Agency, Noordwijk.
- Gough, S. R. 1972. A low temperature dielectric cell and the permittivity of hexagonal ice to 2K. *Can. J. Chem.* **50**, 3046–3051.
- Grard, R. J. L. 1990. A quadrupole system for measuring in-situ the complex permittivity of materials: Application to penetrators and landers for planetary exploration. *Meas. Sci. Technol.* **1**, 806–810.
- Grasset, O., and C. Sotin 1996. The cooling rate of a liquid shell in Titan's interior. *Icarus* **123**, 101–112.
- Johari, G. P., and P. A. Charette 1975. The permittivity and attenuation in polycrystalline and single-crystal ice 1h at 35 and 60 MHz. *J. Glaciol.* **14**, 293–303.
- Jones, T. D., and J. S. Lewis 1987. Estimated impact shock production of N₂ and organic compounds on early Titan. *Icarus* **72**, 381–393.
- Kargel, J. S., S. K. Croft, J. I. Lunine, and J. S. Lewis 1991. Rheological properties of ammonia–water liquids and crystal–liquid slurries: Planetological applications. *Icarus* **89**, 93–112.
- Lamb, J., and A. Turney 1949. The dielectric properties of ice at 1.25 cm wavelength. *Proc. Phys. Soc. (London) B* **62**, 272–273.
- Lewis, J. S. 1973. Interior and its implications for the atmosphere. In *The Atmosphere of Titan* (D. M. Hunten, Ed.), pp. 53–71. NASA SP-340.
- Lorenz, R. D. 1996. Pillow lava on Titan: Expectations and constraints on cryovolcanic processes. *Planet. Space Sci.* **44**, 1021–1028.
- Lorenz, R. D., and J. I. Lunine 1997. Titan's surface reviewed: The nature of bright and dark terrain. *Planet. Space Sci.* **45**, 981–992.
- Lunine, J. I. 1989. Origin and evolution of outer Solar System atmospheres. *Science* **245**, 1417.
- Lunine, J. I., and D. J. Stevenson 1987. Clathrate and ammonia hydrates at high pressure: Application of the origin of methane on Titan. *Icarus* **70**, 61–77.
- Maetzler, C. 1998. Microwave properties of ice and snow. In *Solar System Ices* (B. Schmitt, C. De Bergh, and M. Festou, Eds.), pp. 241–257. Kluwer Academic, Dordrecht.
- Maetzler, C., and U. Wegmuller 1987. Dielectric properties of fresh-water ice at microwave frequencies. *J. Phys. D. (Appl. Phys.)* **20**, 1623–1630.
- Pollack, J. B., A. S. Grossman, R. Moore, and H. R. Graboske, Jr. 1976. The formation of Saturn's satellites and rings, as influenced by Saturn's contraction history. *Icarus* **29**, 35–48.
- Prinn, R. G., and B. Fegley, Jr. 1981. Kinetic inhibition of CO and N₂ reduction in circumplanetary nebulae: Implications for satellite composition. *Astrophys. J.* **249**, 308–317.
- Schmitt, B., E. Quirico, F. Trotta, and W. M. Grundy 1998. Optical properties of ices from UV to infrared. In *Solar System Ices* (B. Schmitt, C. De Bergh, and M. Festou, Eds.), pp. 241–257. Kluwer Academic, Dordrecht.
- Spilker, T. R. 1990. *Laboratory Measurements of Microwave Absorptivity and Refractivity Spectra of Gas Mixtures Applicable to Giant Planet Atmospheres*. Ph.D. dissertation, Stanford University.
- Thompson, W. R., and S. W. Squyres 1990. Titan and other icy satellites: Dielectric properties of constituent materials and implications for radar sounding. *Icarus* **86**, 336–354.
- Tomasko, M. G., L. R. Dose, P. H. Smith, R. A. West, L. A. Soderblom, M. Combes, B. Bezaud, A. Coustenis, C. deBergh, E. Lellouch, J. Rosenqvist, O. Saint-Pe, B. Schmitt, H. U. Keller, N. Thomas, and F. Gliem 1997. The descent imager/spectral radiometer (DISR) aboard Huygens. In *Huygens: Science, Payload and Mission* (A. Wilson, Ed.), pp. 109–138. ESA SP-1177, European Space Agency, Noordwijk.
- Warren, S. G. 1984. Optical constants of ice from the ultraviolet to the microwave. *Appl. Opt.* **23**, 1206–1223.